A BI-LEVEL FREQUENCY SETTING AND PASSENGER ASSIGNMENT MODEL FOR COMPLYING WITH PANDEMIC CAPACITY LIMITS

Konstantinos Gkiotsalitis, Ph.D., Corresponding Author
Assistant Professor
University of Twente, the Netherlands
k.gkiotsalitis@utwente.nl

Oded Cats, Ph.D.
Associate Professor
Delft University of Technology, the Netherlands
o.cats@tudelft.nl

ABSTRACT

Pubic transport is one of the most impacted sectors by the COVID-19 pandemic. Public transport services have experienced a reduction in passenger demand. Notwithstanding this, the social distancing regulations that require public transport service providers to operate under reduced passenger loads stretch the available operational resources. As a consequence, there is an urgent need for new public transport planning tools that can adapt the service supply to the passenger demand. This study proposes a bi-level model for setting the frequencies of public transport lines while accounting for the reduced vehicle capacities due to the pandemic. The upper-level model is a mixed-integer quadratic programming model that sets the line frequencies while accounting for the in-vehicle crowding, whereas the lower-level model is a nonlinear model that performs a probabilistic user-equilibrium passenger assignment. We demonstrate the benefits of our approach for two bus lines in Twente, the Netherlands, using smart card data from the early stages of the pandemic.

INTRODUCTION

Public transport is one of the most affected sectors by COVID-19 in the transportation ecosystem. During the first wave of the pandemic, public transport service providers around the world encountered a major reduction in passenger demand that was as much as 80%-90% in major cities in China, Iran and the United States, and as much as 70%-85% in Europe and the United Kingdom (*1, 2*). This initial ridership drop was a result of changes in travelers' behavior, government regulations, and shifts in work practices, including home office (*3–5*). After the first pandemic wave and the strict lockdowns implemented in countries around the world, there is an incessant alteration between easing and tightening the travel restriction measures based on the transmission rates of COVID-19. At a high level, we have two distinctively different phases in the public transport sector, as described in the review studies of (*6*) and (*7*):

    (1) the strict lockdown phase where travel is reduced to essential trips only;

    (2) the easing phase where travel restrictions are revoked, but passengers should still comply with social distancing rules when inside closed spaces - including public transport vehicles.

       In the strict lockdown phase, the passenger demand is drastically reduced and the public transport service providers are heavily subsidized to continue offering a minimum level of service. In the easing phase, the increase of travel demand poses a considerable challenge to public transport service providers that need to comply with the pandemic-imposed capacity regulations without having the appropriate resources. There are several examples where the public transport sector is scrutinized as one sector that potentially leads to an increase of virus transmissions because public transport service providers cannot ensure that the passenger loads inside vehicles remain below a safe level (*6, 8*). In this study, we call the maximum in-vehicle passenger load that is allowed due to the COVID-19 restrictions *pandemic-imposed capacity*. The pandemic-imposed capacity can be significantly lower than the nominal capacity of a public transport vehicle and might lead to a high number of unserved passengers who are not allowed to board public transport vehicles; thus, resorting to private means of transportation (*9, 10*).

       This study focuses explicitly on the ongoing easing phase of the lockdown where the public transport travel demand increases and the available supply might not be enough to ensure that the pandemic-imposed capacity is maintained during peak times of the day. Our approach introduces a bi-level frequency setting and passenger assignment model that distributes the available vehicles to public transport lines in an optimal way taking into consideration the pandemic-imposed capacity.

       The remainder of this study is structured as follows: in section 2 we present the past literature and the contribution of the study. In section 3 we introduce our bi-level network-wide frequency setting model that considers the pandemic-imposed capacity. In section 4 we introduce our case study and we perform experiments using smart card data from two bus lines in Twente, the Netherlands. Finally, section 5 concludes our work and provides future research directions.

LITERATURE REVIEW

Frequency setting models set the optimal service frequencies of public transport lines based on the trade-off between the passenger-related costs (i.e., passenger waiting times and in-vehicle crowding) and the operational costs (i.e., number of vehicles and drivers needed to operate the service) - see (*11–15*). Of particular interest are analytic approaches that determine the frequency of a single service line based on capacity-related constraints, such as the maximum load point method (*16*). In the maximum load point method, the frequency of a service line within a time period with homo-

geneous passenger demand can be easily determined by dividing the total load of passengers at the stop with the highest load by the capacity of the available vehicles. This results in a closed-form expression and the optimal service frequency can be graphically determined by plotting the total passenger load at each stop. Although the maximum load point method is intuitive and easy to use, there are more comprehensive mathematical models in past literature that try to set the optimal frequencies based on several criteria.

The works of (*17, 18*) consider several criteria, but focus solely on setting the frequency of a single public transport line. Yu et al. (*11*) proposed a genetic algorithm metaheuristic to approximate the solution of the frequency setting problem considering the objective of minimizing the total travel time of passengers subject to fleet size limitations. Sun and Szeto (*19*) introduced a bi-level program to optimize fare and frequency settings. To solve their problem, they proposed a sensitivity-based descent search solution method. Bertsimas et al. (*20*) focused also on the joint frequency setting and pricing optimization problem. They developed formulations for minimizing the system's waiting time in multimodal networks while accounting for operator budget constraints, capacity constraints, and passenger preferences.

Cipriani et al. (*21*) considered the joint problem of frequency setting and route design. Because of the complexity of their problem formulation, they resorted to heuristics such as genetic algorithms for finding a sub-optimal set of routes and line frequencies. Combining the route design and frequency setting problems covers both the network design phase, which is part of strategic planning, and the frequency setting phase, which belongs to tactical planning (*22*). Szeto and Wu (*12*) and Szeto and Jiang (*23*) have also studied this problem with the use of a genetic algorithm in the former study and an artificial bee colony metaheuristic in the latter study. A genetic algorithm was also used by (*24*) and (*25*) that tackled the same problem. Finally, recent approaches have tried to alter the pre-defined routes of public transport lines when setting the service frequencies resulting in short-turning lines that may skip a number of stops (*26–29*).

Past studies have also considered the impact of passenger demand variations in the mathematical formulation of the frequency setting problem. Gkiotsalitis and Cats (*30*) proposed a mathematical model and a solution approach combining branch and bound with sequential quadratic programming to solve the frequency setting problem in the case of travel time and passenger demand uncertainty. Li et al. (*31*) considered also stochastic demand, travel times, and boarding/alighting times by employing a metaheuristic to compute an approximate solution. The passenger demand and dwell time variations were also considered in the work of (*32*).

Summarizing the relevant literature, it is evident that there are five broad categories relevant to our problem: (i) analytic frequency setting methods for single lines, (ii) mathematical programming frequency setting methods for single lines, (iii) frequency setting and fare/pricing optimization approaches, (iv) frequency setting and network design approaches, and (v) stochastic frequency setting approaches that consider the variations of travel times and passenger demand. The closest prior arts to our work are past studies that belong to categories (ii) and (iii) since we also propose a mathematical model for frequency setting while considering additional decision variables from the passenger demand-side. In contrast to the approaches employed in (ii) and (iii), our problem formulation does not focus solely on the trade-off between revenues and operational costs but it also incorporates the pandemic-imposed capacity due to COVID-19. The specific contributions of our study are as follows:

1. the development of a bi-level model that comprises of a scalable mixed-integer quadratic programming model for the frequency setting problem that accounts for the pandemic-

imposed capacity (upper-level), and a probabilistic nonlinear programming model for the passenger assignment (lower-level);
2. the investigation of the improvement potential from the implementation of the proposed approach in two bus lines in Twente, the Netherlands, using smart card data from the pandemic era.

NETWORK-WIDE FREQUENCY SETTING MODEL THAT CONSIDERS PHYSICAL DISTANCING

We model the network-wide frequency setting problem that considers social distancing as a bi-level problem. The upper-level model determines the optimal network-wide line frequencies considering social distancing by minimizing the vehicle deployment costs and the revenue losses due to un-served passengers, and the lower-level model gives an equilibrium passenger demand distribution across different lines by minimizing the expected total travel time of passengers. This interaction game can be represented in a general form as the following bi-level programming problem:

$$(\mathscr{U}_0) \qquad\qquad\qquad \min_{x} \quad F(x,y) \qquad\qquad\qquad (1)$$

$$\text{s.t.} \quad G(x,y) \leq 0 \qquad\qquad\qquad (2)$$

where $y = y(x)$ is implicitly defined by:

$$(\mathscr{L}_0) \qquad\qquad\qquad \min_{y} \quad f(x,y)$$

$$\text{s.t.} \quad g(x,y) \leq 0$$

The bi-level programming model consists of two sub-models: $\mathscr{U}_0$ which is defined as the upper-level problem and $\mathscr{L}_0$ which is the lower level. $F(x,y)$ is the objective function of the upper level decision-maker (public transport service provider) that has x as a decision vector. $G(x,y)$ is the constraint set of the upper-level decision vector. In our case, this constraint set is the expected hourly passenger demand $B^t_{l,r,sy}$ at hour t for passengers of user group r that travel from the origin stop s to the destination stop y using service line l. The values of $B^t_{l,r,sy}$ are determined by solving the lower-level passenger assignment problem. $f(x,y)$ is the objective function of lower-level decision-makers (passengers), y is their decision vector (response function), and $g(x,y)$ is the constraint set of the lower-level decision vector (in our case, this constraint set refers to the optimal frequencies f_l of each service line l that are determined by the upper-level model). This response function connects the upper and lower-level decision variables by solving the models iteratively until convergence (Fig.1).
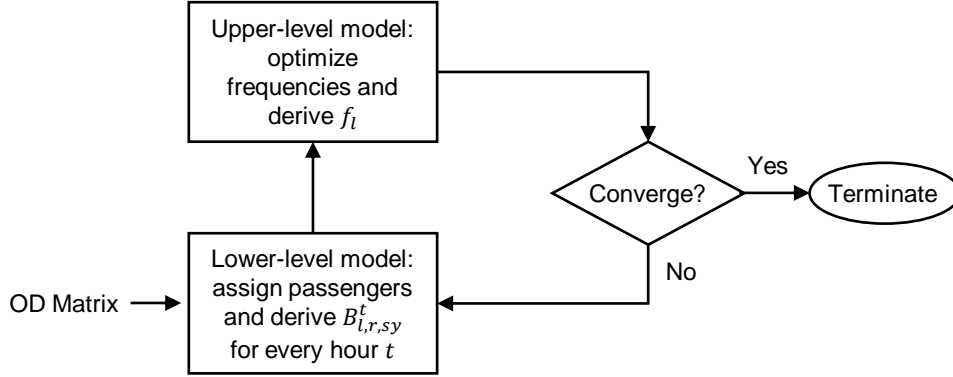
FIGURE 1 Process diagram of the bi-level network-wide frequency setting model embedding a user equilibrium assignment model.

We proceed with presenting first the upper-level network-wide frequency setting model that considers social distancing (section 3.1) followed by the lower-level passenger assignment model (section 3.2).

Upper-level Model: Network-wide Frequency Setting

Let us consider a set of lines $L = \{1, ..., l, ..., |L|\}$ operating in a public transport network (e.g., bus network). Each line l serves a number of bus stops $S_l = \{1, 2, ..., |S_l|\}$. In the upper-level problem, we set the frequencies of all service lines for a time period P which can be a morning period, an afternoon period, or an evening period. Time period P is typically longer than one hour because service lines do not change frequencies so often. A time period P typically consists of multiple hourly sub-periods $t \in P$ that operate under the same frequency but might exhibit different passenger demand levels. In the upper-level model, we use as input the hourly passenger demand $B_{l,r,sy}^t$ for any origin-destination pair s, y of user group r that uses line $l \in L$ for any hour $t \in P$. The line-specific passenger demand $B_{l,r,sy}^t$ for every hour $t \in P$ is determined by solving the lower-level passenger assignment problem described in section 3.2. Before introducing our nomenclature, we list the main assumptions of our study:

(1) The passenger arrival rate is stable within each 1-hour period of the day. That is, passenger arrivals at stations are uniformly distributed within each 1-hour period (a common assumption used by the maximum load point method and (*17, 33, 34*)).

(2) Public transport service providers should offer at least a minimum level of service, e.g., one trip per hour, even if the passenger demand of a service line is very low due to COVID-19.

Note that the focus of this study is on bus networks because our case study involves two high-demand bus lines. The detailed nomenclature of the upper-level network-wide frequency setting model that considers the pandemic-imposed capacity is presented in Table 1.

TABLE 1 Nomenclature

Sets

$L = \langle 1, ..., l, ...|L| \rangle$	set of public transport lines
$R = \langle 1, ..., r, ...|R| \rangle$	set of user groups that use the public transport services (e.g., students, adults, elderly)
$S_l = \langle 1, 2, ..., |S_l| \rangle$	ordered set of public transport stops served by line $l \in L$ (note that a bi-directional line is considered as a single line that continues its service in the opposite direction)
$P = \langle 1, 2, ..., t, ... \rangle$	set of hourly time periods $t \in P$ that operate under the same frequency. The upper-level model seeks to find the optimal line frequencies for time period P

Parameters

$B_{l,r,sy}^t$	expected hourly passenger demand during hour $t \in P$ of user group $r \in R$ at stop s for passengers whose destination is y and are willing to use line l
T_l	round-trip travel time of line $l \in L$ considering both directions in case of a bi-directional line
k_l	pandemic-imposed capacity limit indicating the maximum allowed passenger load inside each bus operating in line l
W	cost of deploying an extra bus
M_r	fare price per km traveled for user group $r \in R$
F_r	fixed minimum fare when entering the bus for user group $r \in R$
$d_{l,sy}$	traveling distance between bus stops s and y of line $l \in L$
N	number of available vehicles that can be allocated to all lines
h_l^{min}	minimum headway of line l, where $h_l^{min} > 0$ to ensure that we do not deploy excessively many vehicles to line l resulting in bus bunching
h_l^{max}	maximum possible headway of line l to ensure that the assigned vehicles to line l offer a minimum level of service to passengers

Variables

x_l	number of vehicles assigned to line $l \in L$
h_l	time headway among successive vehicles of line $l \in L$
$\gamma_{l,s}^t$	in-vehicle passenger load of each vehicle serving line l during the t-th hour when it departs from stop s
$b_{l,r,sy}^t$	hourly passenger demand of user group r between stops s and y of line l that can be served by the vehicles of line l while conforming to the pandemic-imposed capacity limits
$b_{l,sy}^t$	aggregated hourly passenger demand of all user groups between stops s and y of line l that can be served by the vehicles of line l while conforming to the pandemic-imposed capacity limits
$\tilde{b}_{l,r,sy}^t$	hourly passenger demand of user group r between stops s and y of line l that cannot be accommodated by line l due to the pandemic-imposed capacity limit k_l
f_l	service frequency of line $l \in L$

To derive the optimal allocation of vehicles to service lines, we use the following hierarchy in the decision-making process:

 (i) if the passenger demand does not exceed the pandemic-imposed capacity limits of vehicles, then our objective is to reduce the number of assigned vehicles as much as possible. This minimizes the operational costs while ensuring that a minimum level of service is guaranteed. In this case, the minimum level of service is guaranteed by not allowing the

line headways to exceed h_l^{max}, $\forall l \in L$.

(ii) if the passenger demand exceeds the pandemic-imposed capacity limit of at least one service line, more vehicles will be assigned to the problematic line(s), provided that there are enough additional vehicles in reserve.

(iii) if after assigning the entirety of available vehicles in an optimal way there are still un-served passengers, then our objective is to reduce the number of unserved passengers and the corresponding revenue losses for the public transport service provider.

Formally, to reduce the number of deployed vehicles as much as possible and mitigate the operational costs according to objective (i), we would need to solve the following program:

$$(\mathscr{U}_1) \quad \min W \sum_{l \in L} x_l \tag{3}$$

$$\text{s.t.} \sum_{l \in L} x_l \leq N \tag{4}$$

$$h_l x_l \geq T_l, \quad \forall l \in L \tag{5}$$

$$h_l \leq h_l^{max}, \quad \forall l \in L \tag{6}$$

$$h_l \geq h_l^{min}, \quad \forall l \in L \tag{7}$$

Eq.(3) strives to minimize the total number of assigned vehicles to all lines $l \in L$. The inequality constraint (4) ensures that we cannot deploy more vehicles to lines than the maximum number of available vehicles, N. Constraint (5) ensures that the time headway of each line $l \in L$ should be at least greater than T_l/x_l, where T_l is the round-trip travel time of line l and x_l the number of assigned vehicles to that line. Constraint (6) ensures that the planned headway of each line is less than or equal to h_l^{max} to offer a minimum level of service by not letting passengers waiting at stops for excessive periods of time. Finally, constraint (7) prohibits bunching by guaranteeing a minimum headway among buses of the same line.

Note that formulation $(\mathscr{U}_1)$ does not consider the passenger demand, the in-vehicle pas-senger loads, and the pandemic-imposed vehicle capacities. According to objective (ii), our model should be forced to use more vehicles when at least one service line does not meet its pandemic-imposed capacity limit. For this, we use the additional constraints:

$$b_{l,r,sy}^t = B_{l,r,sy}^t, \quad \forall l \in L, \forall r \in R, \forall s \in S_l, \forall y \in S_l \mid y \geq s, \forall t \in P \tag{8}$$

$$b_{l,sy}^t = \sum_{r \in R} b_{l,r,sy}, \quad \forall l \in L, \forall s \in S_l, \forall y \in S_l \mid y \geq s, \forall t \in P \tag{9}$$

$$\gamma_{l,1}^t = \sum_{y \in S_l} b_{l,1y}^t h_l, \quad \forall l \in L, \forall t \in P \tag{10}$$

$$\gamma_{l,s}^t = \gamma_{l,s-1}^t - \sum_{\substack{y \in S_l \\ y < s}} b_{l,ys}^t h_l + \sum_{\substack{y \in S_l \\ y > s}} b_{l,sy}^t h_l, \quad \forall l \in L, \forall s \in S_l \setminus \{1\}, \forall t \in P \tag{11}$$

$$\gamma_{l,s}^t \leq k_l, \quad \forall l \in L, \forall s \in S_l, \forall t \in P \tag{12}$$

Constraint (8) sets the hourly passenger demand of user group r between stops s and y of line l that conforms with the pandemic-imposed capacity limit ($b_{l,r,sy}^t$) equal to the expected hourly

passenger demand, $B^t_{l,r,sy}$, that is computed by the lower-level passenger assignment model. As we will later show, it might not be possible to serve all demand $B^t_{l,r,sy}$ given the pandemic-imposed capacity resulting in the subsequent amendment of constraint (8). Constraint (9) computes the aggregated hourly demand from stop s to y of line l that conforms with the pandemic-imposed capacity limit. Constraint (10) determines the in-vehicle passenger load when a vehicle departs from the terminal. This is the number of passengers that board at stop 1 and will alight at any other stop y within our 1-hour time period, $b^t_{l,sy}$, multiplied by the time headway among successive trips, h_l, since we refer to the passenger load of individual vehicles. Similarly, the recursive equation (11) determines the in-vehicle passenger load when a vehicle of line l departs from stop $s \in S_l \setminus \{1\}$. This equation is the passenger flow conservation equation where the in-vehicle passenger load for vehicles operating during the t-th hour is equal to the passenger load when departing from the previous stop, $\gamma^t_{l,s-1}$, minus the number of passengers that alight at stop s, $\sum_{\substack{y \in S_l \\ y < s}} b^t_{l,ys} h_l$, plus the number of passengers that board at stop s and will alight at any other stop $y > s$ of line l. Note that $\sum_{\substack{y \in S_l \\ y<s}} b^t_{l,ys} h_l$ is the sum of the time headway multiplied by the hourly passenger demand that enters line l at any stop $y \in S_l \mid y < s$ and exits at stop s. Finally, constraint (12) requires that the in-vehicle passenger load should not exceed the pandemic-imposed capacity at any stop.

The mathematical program in Eqs.(3)-(12) assigns vehicles x_l to lines $l \in L$ such that the total number of deployed vehicles is minimized (objective i), whereas the in-vehicle passenger load remains below the pandemic imposed capacity limit (objective ii). This mathematical program, however, is not always feasible. Indeed, if the passenger demand values that are derived by the lower-level passenger assignment model $(B^t_{l,r,sy})$ are high, then constraint (8) will lead to a prohibitively high value of $b^t_{l,r,sy}$ that can result in the violation of the pandemic-imposed capacity constraint (12). To ensure that the pandemic-imposed capacity constraint (12) is always satisfied, we need to transform the mathematical program into a feasible one by relaxing constraint (8). To this end, constraint (8) is substituted by:

$$b^t_{l,r,sy} = B^t_{l,r,sy} - \tilde{b}^t_{l,r,sy} \qquad\qquad \forall l \in L, \ \forall r \in R, \ \forall s \in S_l, \ \forall y \in S_l \mid y \geq s, \forall t \in P \qquad (13)$$

where $\tilde{b}^t_{l,r,sy} \geq 0$ is the unserved passenger demand of user group r that was willing to travel from stop s to stop y of line l during hour t. This unserved passenger demand in constraint (13) reduces the value of the actually served passenger demand, $b^t_{l,r,sy}$, which becomes the portion of the overall demand $B^t_{l,r,sy}$ that can be served by line l without violating the pandemic-imposed capacity constraint of Eq.(12). Constraint (13) has a prominent role in our mathematical program because it ensures feasibility. However, it also indicates that the overall demand $B^t_{l,r,sy}$ cannot be always served. If one assumes that the unserved passengers are uniformly distributed across all user groups following a first-come, first-served boarding process, then an additional constraint $b^t_{l,r,sy} = \frac{B^t_{l,r,sy}}{\sum_{r \in R} B^t_{l,r,sy}} b^t_{l,sy}$ should be added in case of $\tilde{b}^t_{l,r,sy} > 0$ to ensure that each user group will have the same number of unserved passengers.

Replacing constraint (12) by constraint (13) introduces an unserved passenger demand that our mathematical program should keep to a minimum. This is part of objective (iii) which strives to minimize the revenue losses because of unserved passenger demand. These revenue losses appear

only in the case that assigning all available vehicles is not enough to maintain the passenger loads below the pandemic-imposed capacity. To this end, we add a penalty to the objective function that prioritizes the minimization of the revenue losses due to unserved demand over the operational costs related to the number of assigned vehicles. The objective function presented in Eq.(3) is therefore reformulated as:

$$\min \; W \sum_{l \in L} x_l + \sum_{t \in P} \sum_{l \in L} \sum_{r \in R} \sum_{\substack{s \in S_l \\ s \neq |S_l|}} \sum_{\substack{y \in S_l \\ y > s}} (F_r + M_r d_{l,sy}) \tilde{b}^t_{l,r,sy} \tag{14}$$

where $\sum_{t \in P} \sum_{l \in L} \sum_{r \in R} \sum_{\substack{s \in S_l \\ s \neq |S_l|}} \sum_{\substack{y \in S_l \\ y > s}} (F_r \tilde{b}^t_{l,r,sy} + M_r d_{l,sy} \tilde{b}^t_{l,r,sy})$ is the penalty term indicating the revenue losses because of the unserved passengers. In more detail, when a passenger enters the vehicle he/she pays a fixed minimum fare F_r depending on his/her user group r and an additional fare $M_r d_{l,sy}$ depending on the distance traveled, $d_{l,sy}$, until the passenger exits the vehicle. If we have $\tilde{b}^t_{l,r,sy}$ unserved passengers of group r that were willing to travel from stop s to stop y of line l, then the public transport service provider will lose a revenue of $F_r \tilde{b}^t_{l,r,sy}$ from the fixed fares collected when passengers enter the vehicle and $M_r d_{l,sy} \tilde{b}^t_{l,r,sy}$ from the additional fares that depend on the distance that any unserved passengers would have traveled. Adding all the revenue losses due to the unserved passengers of every user group $r \in R$ traveling from any stop $s \in S_l \mid s \neq |S_l|$ to any stop $y \in S_l \mid y > s$ of any line $l \in L$ results in the total revenue losses of $\sum_{t \in P} \sum_{l \in L} \sum_{r \in R} \sum_{\substack{s \in S_l \\ s \neq |S_l|}} \sum_{\substack{y \in S_l \\ y > s}} (F_r \tilde{b}^t_{l,r,sy} + M_r d_{l,sy} \tilde{b}^t_{l,r,sy})$.

Summarizing our previous transformations, our mathematical program that assigns the optimal number of vehicles to each line in order to determine the service frequencies while considering the pandemic-imposed capacities is presented below:

$$(\mathscr{U}_2) \quad \min W \sum_{l \in L} x_l + \sum_{t \in P} \sum_{l \in L} \sum_{r \in R} \sum_{\substack{s \in S_l \\ s \neq |S_l|}} \sum_{\substack{y \in S_l \\ y > s}} (F_r + M_r d_{l,sy}) \tilde{b}^t_{l,r,sy} \tag{15}$$

$$\text{s.t.} \sum_{l \in L} x_l \leq N \tag{16}$$

$$h_l x_l \geq T_l, \quad \forall l \in L \tag{17}$$

$$h_l^{min} \leq h_l \leq h_l^{max}, \quad \forall l \in L \tag{18}$$

$$\gamma^t_{l,s} \leq k_l, \quad \forall l \in L, \forall s \in S_l, \forall t \in P \tag{19}$$

$$\gamma^t_{l,1} = \sum_{y \in S_l} b^t_{l,1y} h_l, \quad \forall l \in L, \forall t \in P \tag{20}$$

$$\gamma^t_{l,s} = \gamma^t_{l,s-1} - \sum_{\substack{y \in S_l \\ y < s}} b^t_{l,ys} h_l + \sum_{\substack{y \in S_l \\ y > s}} b^t_{l,sy} h_l, \quad \forall l \in L, \forall s \in S_l \setminus \{1\}, \forall t \in P \tag{21}$$

$$b^t_{l,r,sy} = B^t_{l,r,sy} - \tilde{b}^t_{l,r,sy}, \quad \forall l \in L, \forall r \in R, \forall s \in S_l, \forall y \in S_l \mid y \geq s, \forall t \in P \tag{22}$$

$$b^t_{l,sy} = \sum_{r \in R} b^t_{l,r,sy}, \quad \forall l \in L, \forall s \in S_l, \forall y \in S_l \mid y \geq s, \forall t \in P \tag{23}$$

$$x_l \in \mathbb{Z}_{\geq 0}, \quad \forall l \in L \tag{24}$$

$$h_l \in \mathbb{R}_{\geq 0}, \quad \forall l \in L \tag{25}$$

Remark 1. Mathematical program ($\mathscr{U}_2$) is a mixed-integer quadratic program (MIQP) because its objective function is linear and it has linear and quadratic constraints. The quadratic constraints are constraints (20) and (21) related to the calculation in the in-vehicle passenger load at each stop.

Remark 2. To force our model to use additional vehicles when we have unserved demand, the importance of the revenue losses term in our objective function should be greater than the importance of the operational costs, $W \sum_{l \in L} x_l$. To achieve this, the weight factor W that indicates the cost of deploying extra vehicles should be sufficiently small.

It is worth noting that program ($\mathscr{U}_2$) returns the optimal number of vehicles x_l and headways h_l for each service line $l \in L$. From this, we can easily determine the optimal frequency of each line as $f_l = 1/h_l$.

Lower-level Model: Passenger Assignment
The lower-level model considers the line frequencies $f_l = 1/h_l \ \forall l \in L$ that are determined by the upper-level model as fixed input. An additional input to the lower-level model is the hourly OD matrix $O^t_{r,sy}, \ \forall t \in P$. For each hour $t \in P$, the lower-level model will determine the passenger demand assignment to lines $B^t_{l,r,sy}$. The decision makers at the lower-level are the passengers and their objective is to minimize their individual trip travel time (including the in-vehicle riding times and the waiting times at stops, including when transferring). For the lower-level problem, we consider an adapted version of the seminal passenger assignment model of (*35*).

Passenger trips are split into trip components that are represented by arcs $a \in A$ in a network $G = (I, A)$. The trip components $a \in A$ are not necessarily inter-station links. Trip components can be boarding links, alighting links, walking links and in-vehicle traveling links. For instance, a trip component can be a waiting time, a transfer time or a riding time when using a vehicle of a

particular service line. In this network representation, $i \in I$ are vertices that have incoming and outgoing trip components (arcs). Note that we might have multiple vertices in the same physical location because at that location there might be different travel options for a passenger that seeks to arrive at his/her final destination. Let A_i^+ be the set of outgoing arcs from vertex i and A_i^- the set of incoming arcs. Each arc a has a travel time $c_a \geq 0$. For arcs that represent a boarding or alighting, $c_a = 0$. In addition, arcs have frequencies $f_a \in [0, +\infty]$ and waiting times $w_a \in [0, +\infty]$. Because each arc a is a trip component, it is associated with one, and only one, service line l. For instance, if arc a is part of line l, then the frequency of this arc is $f_a = f_l$ if arc a is related to the boarding trip component to line l. If, however, arc a is an alighting or an in-vehicle riding arc, then $f_a = +\infty$ and $w_a = 0$ because passengers do not experience any waiting time when using this trip component. To summarize, three types of trip components are considered:

- waiting for boarding trip component ($c_a = 0$, $f_a > 0$, $w_a > 0$),
- in-vehicle riding trip component ($c_a > 0$, $f_a = +\infty$, $w_a = 0$),
- alighting trip component ($c_a = 0$, $f_a = +\infty$, $w_a = 0$).

Note that the alighting trip component has not travel cost and no waiting cost. The boarding trip component has waiting cost but no on-board travel cost, and the in-vehicle riding trip component has an on-board travel cost but no waiting cost. It is also worth stressing again that the frequency of a boarding trip component, f_a, is equal to f_l, where l is the corresponding line l to arc a. That is, the f_a values are a direct input from the upper-level model (parameters).

The passenger volume traversing vertex i is given by:

$$v_i = \sum_{a \in A_i^-} v_a + g_i \quad \forall i \in I \tag{26}$$

where g_i is the demand in vertex i and v_a is the passenger volume of arc $a \in A_i^-$. For modeling purposes, let parameter $\mu_{a,i} = 1$ if arc a is an outgoing arc of vertex i and $\mu_{a,i} = 0$ otherwise. Let also $\lambda_{a,i} = 1$ if arc a is an incoming arc of vertex i and 0 otherwise. Then, the probability $\mathscr{P}_{a,i}$ of using arc a among all outgoing arcs A_i^+ from vertex i is:

$$\mathscr{P}_{a,i} := \frac{f_a \mu_{a,i}}{\sum\limits_{a' \in A} f_{a'} \mu_{a',i}} \quad \forall a \in A \tag{27}$$

Note that $\mathscr{P}_{a,i} = 0$ if a is not an outgoing arc of vertex i, because then $\mu_{a,i} = 0$. This probability dictates a probabilistic passenger assignment among different arcs with passengers having a higher probability to use the arcs of lines with higher frequencies that will result in lower waiting times. In particular, the vertex volume v_i will be distributed to the outgoing arcs of vertex i according to their arc probabilities, $v_a = \mathscr{P}_{a,i} v_i$.

In addition, the expected combined waiting time ω_i for passengers waiting at vertex i is:

$$\omega_i := \frac{\theta}{\sum\limits_{a \in A} f_a \mu_{a,i}} \quad \forall i \in I \tag{28}$$

where $\theta \geq 0$ is equal to 0.5 the frequency for reliable high-frequency services where services follow a regular arrival pattern and passengers are assumed to not coordinate their arrivals

with the arrival times of vehicles and is equal to 1 for low-frequency and unreliable services. Note that both the assignment probabilities $\mathscr{P}_{a,i}$ and the combined waiting times ω_i have fixed values because f_a and $\mu_{a,i}$ are parameters in the lower-level model. In the assignment, the optimal strategy for all travelers who are willing to reach destination q from any origin vertex is derived by solving the following mathematical program. In this program, the only variables are $v_a \ \forall a \in A$, which denote the passenger volume at arc a, and $w_i \ \forall i \in I$, which denote the total passenger waiting time for all trips at vertex i.

$$(\mathscr{L}_1) \quad \min \quad \sum_{a \in A} c_a v_a + \sum_{i \in I} w_i \tag{29}$$

$$\sum_{a \in A} \mu_{a,i} v_a - \sum_{a \in A} \lambda_{a,i} v_a = g_i \ \ \forall i \in I \setminus \{r\} \tag{30}$$

$$v_a \mu_{a,i} \leq f_a w_i \ \ \forall a \in A, i \in I \tag{31}$$

$$v_a \geq 0 \ \ \forall a \in A \tag{32}$$

$$v_a \in \mathbb{R}_+ \ \ \forall a \in A, \ w_i \in \mathbb{R}_+ \ \ \forall i \in I \tag{33}$$

Program $(\mathscr{L}_1)$ assigns passengers from all origins to destination q to minimize the total travel times at the arcs and the waiting times at vertices. It is a linear program with $|I| \times |A|$ variables (v_a and w_i). For in-vehicle riding and alighting arcs that have frequencies $f_a = +\infty$ we set $f_a = M$, where M is a very large positive number. This avoids multiplications by $+\infty$. Constraint (30) is the passenger flow conservation constraint which ensures that the outgoing flow from all outgoing arcs from vertex i is equal to the incoming flow, $\sum_{a \in A} \lambda_{a,i} v_a$, plus the passenger demand, g_i, at vertex i. Constraint (31) ensures that the passenger volume v_a in the outgoing arc a of vertex i is lower than or equal to the frequency of that arc multiplied by the total waiting time for all trips at vertex i. Note that if a is not an outgoing arc of vertex i constraint (31) is satisfied because the left hand-side is equal to zero. Finally, constraint (32) ensures that the volume traversing an arc cannot be negative.

Formulation $(\mathscr{L}_1)$ assigns the passenger demand probabilistically to different paths, but it does not consider the effect of in-vehicle congestion on the passengers' path selection. This is a shortcoming because passengers might perceive the in-vehicle travel times in crowded vehicles to be higher compared to the ones in less crowded vehicles (*36*). To rectify this, let the arc travel times c_a be no longer constant, but continuous non-decreasing functions of the corresponding arc flows $c_a(v_a)$. By doing so, the assignment problem is no longer separable by destination node. As a result, the optimal assignment strategies can be defined by Wardrop's second principle, implying that only strategies with minimal expected cost will be used by the travelers (*37*). To solve the passenger assignment problem from all origins to all destinations $q \in Q$, we set first subsets of vertices $I_q \subseteq I$ that contain all vertices before destination q. We also set variables $\tilde{v}_{a,q}$ and $w_{i,q}$ indicating the flow in arc a from all passengers traveling to destination q and the waiting time at vertex i for passengers traveling to destination q. Let also $g_{i,q}$ be the demand in vertex i for passengers that travel to destination $q \in Q$. If c_a^0 is the fixed arc travel time without considering any congestion, then the passenger assignment problem that considers in-vehicle crowding can be cast as follows:

$$(\mathscr{L}_2) \quad \min \qquad \underbrace{\sum_{a \in A} c_a^0 v_a + \sum_{q \in Q} \sum_{i \in I} w_{i,q} +}_{\text{actual travel cost}} \underbrace{\sum_{a \in A} c_a^0 \int_0^{v_a} d_a(z)\, dz}_{\text{perceived cost due to congestion}} \qquad (34)$$

$$v_a = \sum_{q \in Q} \tilde{v}_{a,q} \quad \forall a \in A \qquad (35)$$

$$\sum_{a \in A} \tilde{v}_{a,q} \mu_{a,i} - \sum_{a \in A} \tilde{v}_{a,q} \lambda_{a,i} = g_{i,q} \quad \forall\, i \in I_q, q \in Q \qquad (36)$$

$$\tilde{v}_{a,q} \mu_{a,i} \leq f_a w_{i,q} \quad \forall a \in A, i \in I, q \in Q \qquad (37)$$

$$\tilde{v}_{a,q} \geq 0 \quad \forall a \in A, q \in Q \qquad (38)$$

$$\tilde{v}_{a,q} \in \mathbb{R}_+ \ \forall a \in A, q \in Q, \ w_{i,q} \in \mathbb{R}_+ \ \forall i \in I, q \in Q \qquad (39)$$

Note that now the objective function includes the nonlinear term of the additional perceived travel cost due to congestion, where $d_a(z)$ is a continuous non-decreasing function of the corresponding arc flows. Spiess (*38*) proposed a series of conical volume-delay functions for passenger assignment, although one of the most common ones is an adaptation of the Bureau of Public Roads (BPR) function that will result in a $\int_0^{v_a} d_a(z)\, dz$ equal to:

$$\int_0^{v_a} d_a(z)\, dz = \left(\frac{v_a}{f_a \gamma_a} \right)^{\beta} \qquad (40)$$

where v_a is the passenger volume of trip component a, γ_a is the nominal capacity of the line that serves arc a, and β a BPR function parameter that typically takes values in the range $2 \leq \beta \leq 12$ (see (*38*)). If one sets $\beta = 2$, the objective function has a quadratic form.

Remark 3. One additional important point is the inclusion of an additional waiting penalty for passenger transfers, on top of the actual waiting time for the transfer. This penalty can be perceived as extra discomfort due to transferring between lines. To model this, one could provide a frequency penalty $f_a = \varepsilon$, where $0 < \varepsilon < M$, to alighting trip components because any alighting arc that does not end up to the final destination of a passenger will force the passenger to use a subsequent boarding arc to make a transfer.

Fig.2 provides the representation of the multi-line network used in (*38*) using the proposed modeling convention. The left part of the figure presents the actual network with 4 lines and 4 stops. The right part of the network presents the network representation considering the boarding, alighting, and in-vehicle running trip components. All alighting trip components have $(c_a^0, f_a) = (0, M)$ and they are presented with trimmed lines. The in-vehicle trip components have values (c_a^0, M), where $c_a^0 > 0$, and the boarding trip components have values $(0, f_a)$, where $f_a < M$. The frequencies are expressed in vehicles per minute (i.e. 1/6 is a frequency of 10 vehicles per hour).
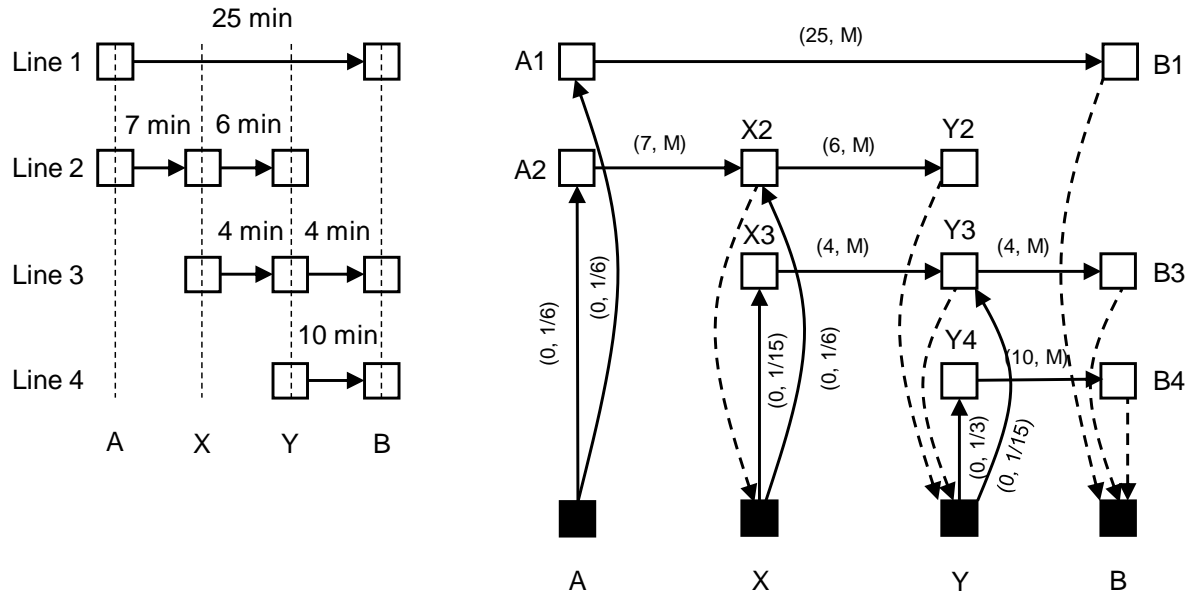
FIGURE 2 Network of Spiess and Florian (*35*). Left: The network with 4 lines and stops A, X, Y and B. Right: Representation of the network where alighting trip components are represented with trimmed lines and they all have travel times and frequencies (0,M).

The results of the lower-level model ($\mathcal{L}_2$) return the passenger demand matrix $B^t_{l,sy}$ per line for every hourly period t and they are used by the upper-level model ($\mathcal{U}_2$) to set the optimal frequency. To summarize, the lower-level model ($\mathcal{L}_2$) and the upper-level model ($\mathcal{U}_2$) are solved in an iterative manner until convergence, as previously described in Fig.1.

MODEL APPLICATION
Case study description
Our case study involves two bus lines in the Twente region in the Netherlands. Although our approach is implemented for two bus lines, it can be implemented to an entire bus network without loss of generality. The two bus lines are operated by Keolis Nederland, which is the public transport service provider in Twente. The selected lines are line 62 and line 2 because they maintained high passenger demand during the pandemic and are impacted by the pandemic-imposed capacity resulting in unserved passengers. Bus line 62 connects the towns of Borculo and Denekamp. It is a long line covering approximately 60 km per direction and serving 74 bus stops per direction (a round-trip of line 62 serves $S_{62} = \{1, 2, ..., 148\}$ bus stops). Bus line 2 is much shorter and operates in the city of Enschede. It covers a distance of approximately 13 km and serves 40 bus stops per direction ($S_2 = \{1, 2, ..., 80\}$ stops for a round-trip). They share a corridor with 7 transfer stops (14 if we consider both directions). The topology of bus lines 62 and 2 is illustrated in Fig.3.
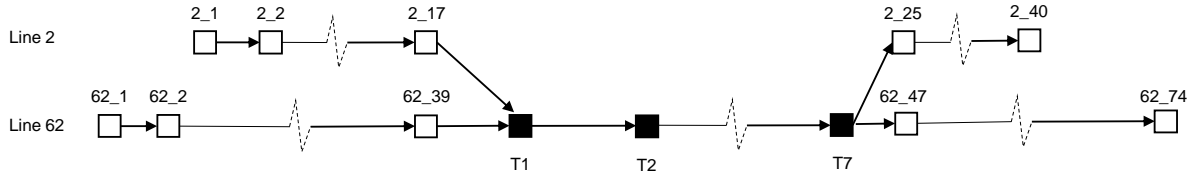
FIGURE 3 Topology of bus line 2 (top) and bus line 62 (bottom). Note that stops 2_18-2_19-...-2_24 of line 2 and stops 62_40-62_41-...-62_46 of line 62 are at the same physical locations, denoted as T1-T2-...-T7.

Using the convention from the passenger assignment model in section 3.2, the topology of Fig.3 results in the network representation of Fig.4 when solving the lower-level passenger assignment problem. In this representation, alighting trip components are represented by trimmed lines. Boarding trip components and in-vehicle riding trip components are presented with solid lines. In addition, the in-vehicle riding and boarding trip components are merged in vertices that have only one incoming and one outgoing arc (that is, in vertices that do not permit transfers). These merges are performed to simplify the network representation. Because of these merges, an arc a, i.e., the arc that connects 2_1 and 2_2, will have a cost $c_a^0 > 0$ equal to the riding cost from 2_1 to 2_2, and a frequency f_a equal to the frequency of line 2.
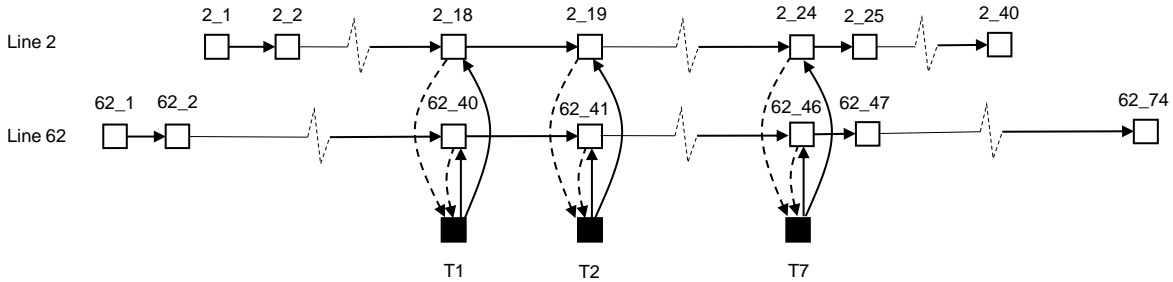

FIGURE 4 Network representation of bus line 2 (top) and bus line 62 (bottom) following the convention of the lower-level model.

Our experiments focus on the time period P from 8 am until 10 am on a Monday in March, 2020. This period is selected because it includes the morning peak hour from 8 am to 9 am, which has a high passenger demand that might lead to unserved passengers due to the pandemic-imposed capacity limit. During this 2-hour period, $P = \langle 1, 2 \rangle$, the round-trip travel time of line 62 is $T_{62} = 210$ minutes and of line 2 is $T_2 = 86$ minutes, considering a layover time of 10 minutes in both cases.

The total number of available buses that can be assigned to these two lines is $N = 16$ and all buses are of the same type with a nominal capacity of $\gamma_a = 38$ seated passengers. To ensure safe distancing among passengers, we consider a pandemic-imposed capacity of $k_l = 15$ passengers for any bus operating in line 62 or 2.

Regarding the user types of passengers, in the Twente region there are six different categories: $R = \{$anonymous travelers; adults; higher-education students; elderly (more than 65 years

old); kids/teenagers; business card holders}. The fixed minimum fare for entering a bus, F_r, and the fare price per km traveled varies for the different user types. The costs are summarized in Table 2 together with the demand share of each user type.

TABLE 2 Minimum fare price, F_r, and additional charging per km traveled, M_r, per user type

	Anonymous	Adults	Higher education students	Elderly	Kids / Teenagers	Business card holders
F_r (€)	0.98	0.98	0.33	0.33	1.10	0.78
M_r (€ per km)	0.202	0.202	0.069	0.069	0.000	0.162
Demand share (%)	15%	24%	44.5%	1.2%	11.5%	3.8%

We note that anonymous users are users that do not have a specific smart card identification and pay the maximum fare - similar to the fare paid by adults. In addition, students might travel for free during certain times of the day and we have selected fare price estimates for the business card holders because they can benefit from various subscription models.

To avoid bus bunching, the bus trips of each bus line should have a minimum time headway of at least $h_l^{min} = 1$ minute. In addition, to ensure a minimum level of service regarding the passenger waiting times at stops, the maximum allowed time headway of line 2 is $h_2^{max} = 15$ minutes and of line 62 is $h_{62}^{max} = 30$ minutes. Note that the maximum time headway of line 62 is twice as long because line 62 connects two towns and it is acceptable to operate under lower frequencies compared to line 2 that serves the core of the city of Enschede, which is the most populous city in the Twente region.

If we do not consider the pandemic-imposed capacity, line 62 can operate during the morning period with a time headway of $h_{62} = 30$ min, equivalent to a frequency of $f_{62} = 2$ vehicles per hour, in order to minimize the operational costs while offering a minimum level of service. To achieve this time headway, we need to assign $x_{62} = \left\lceil \frac{T_{62}}{h_{62}} \right\rceil = 7$ buses to line 62. In addition, line 2 can operate with a time headway of $h_2 = 15$ min and frequency of $f_2 = 4$ vehicles per hour, which is achieved with the allocation of $x_2 = \left\lceil \frac{T_2}{h_2} \right\rceil = 6$ buses. Note that the total number of buses assigned to lines 62 and 2 is 7+6=13, which is less than the total number of available buses, $N = 16$. Given this service supply, we perform a passenger assignment using the lower-level model ($\mathcal{L}_2$) by assuming $\beta = 2$. After assigning passengers to trip components, $a \in A$, Fig.5 presents the number of unserved passengers per stop during the 8-9 am peak in case the pandemic-imposed capacity is implemented for this set of service frequencies. Note that this level of service is considered as the as-is (benchmark) scenario and its performance will be compared against the proposed solutions of our approach. Note also that we present the peak hour from 8 am to 9 am because there are no unserved passengers from 9 am to 10 am when adopting the suggested frequencies.
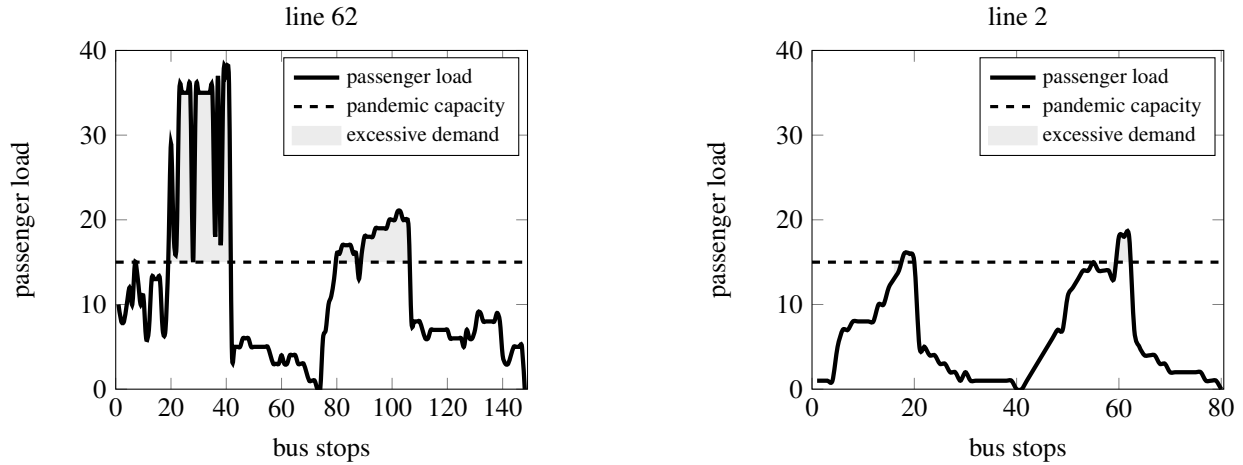
FIGURE 5 Average in-vehicle passenger load from 8 am to 9 am when a bus departs from a stop when line 62 operates with a frequency of $f_{62} = 2$ vehicles per hour and line 2 with a frequency of $f_2 = 4$ vehicles per hour.

From Fig.5 one can note that when catering for operational costs, the seated (nominal) capacity of 38 passengers is sufficient. Notwithstanding this, the pandemic-imposed capacity of 15 passengers is violated with overcrowding for large parts of the routes, especially for buses operating in line 62. In the next sub-section, we demonstrate how our proposed model can assign the available buses to lines in an optimal way that caters for both the operational costs and the pandemic-imposed capacity.

Frequency setting considering the pandemic-imposed capacity
In our case study we implement our lower-level passenger assignment model expressed in our nonlinear program ($\mathscr{L}_2$). This model is programmed in Python and solved with `Gurobi 9.0.3`, which is an optimization solver. The required input for the lower-level model is the frequency of each service line and the OD matrix from 8 am until 9 am and from 9 am until 10 am. Its output is the assignment of passenger trips $B^t_{l,r,sy}$ for the 8-9 am time period and for the 9-10 am time period.

In addition, we implement our upper-level frequency setting model ($\mathscr{U}_2$) that accounts for the pandemic-imposed capacity. This MIQP is programmed in Python and it is solved using `Gurobi 9.0.3`, which can solve mixed-integer quadratically constrained problems. The outcome of the solver is the optimal assignment of buses x_{62}, x_2 and the respective line frequencies f_{62}, f_2 for the time period 8 am to 10 am. This outcome is used from the lower-level model to conduct a new passenger assignment until the results stabilize (see the bi-level optimization process in Fig.1).

To solve the upper-level model with `Gurobi 9.0.3` for the planning period P, we tested in a pre-calibration phase different values for the parameter W to ensure that meeting the pandemic-imposed capacity is more important than reducing the number of deployed vehicles. After initial experiments, we set the value of W to 0.001 because it satisfied this criterion for the data of our case study.

Concerning the computation of an optimal solution, the lower-level LP model has only continuous variables and is solved almost immediately, whereas the upper-level MIQP model has two integer variables and is solved in, approximately, 1 second for the case of two lines. The resulting optimal frequency setting solution for the time period 8 am - 10 am after implementing

the bi-level optimization are:

- optimal frequencies: line 62 $f_{62} = 2.86$ veh per hour, line 2 $f_2 = 4$ veh per hour.
- optimal number of buses: line 62 $x_{62} = 10$, line 2 $x_2 = 6$.
- optimal headways: line 62 $h_{62} = 21$ min, line 2 $h_2 = 15$ min.

The resulting passenger load at each stop when implementing our solution during the peak hour 8-9 am is presented in Fig.6. Fig.6 offers a considerable improvement in terms of satisfying the pandemic-imposed capacity compared to the results of the solution in Fig.5 that did not account for the pandemic capacity. In more detail, it reduces the number of unserved passengers from 59 to 42 (29% decrease) during the 1-hour period from 8 am to 9 am. This improvement in terms of unserved passengers requires the addition of 3 extra buses, but this extra operational cost is justifiable given the reduction of the in-vehicle crowding levels.
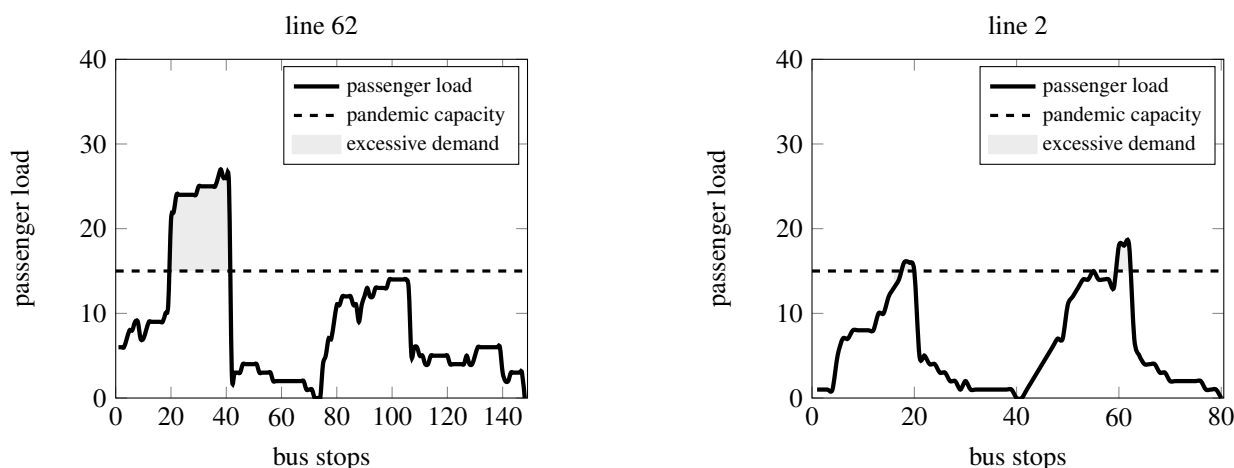

FIGURE 6 Average in-vehicle passenger load when a bus departs from a stop when line 62 operates with a headway of $h_{62} = 21$ minutes and line 2 with a headway of $h_2 = 15$ minutes for the peak hour 8-9 am.

One final note is that our solution's results in Fig.6 cannot satisfy the passenger demand at all stops during the 8 am - 9 am peak, resulting in unserved passengers. The line segment from stop 20 until stop 40 of line 62 is especially problematic. The reason behind this is that even if we deploy all $N = 16$ available buses, this is not sufficient to accommodate all passengers given the pandemic-imposed capacity.

CONCLUSION

This study proposed a novel bi-level optimization model for setting the frequencies of public transport lines based on the pandemic-imposed capacity limitations. The upper-level, mixed-integer quadratic programming model developed in this study was applied to two high-demand bus lines in Twente, the Netherlands. To produce the line-level passenger demand for the upper-model, a lower-level probabilistic passenger assignment model was used following a nonlinear programming formulation. Results from our analysis showed that our approach yields a service plan that performs better than the benchmark service plan that sets the service frequencies without considering the COVID-19 restrictions resulting in 29% less unserved passengers. Our study is applied

to two bus lines, but it can be implemented for an entire public transport network without loss of generality.

In future research, one could expand our approach to consider larger networks with a mixture of bus and train lines. In addition, similarly to the vast majority of past studies in frequency settings, our approach assumes that the passenger demand is uniformly distributed across small discretized time periods of 1 hour. Different tests can be implemented by reducing this time period (e.g., considering 15 or 30-minute intervals of homogeneous passenger demand) to capture the effect of demand peaks with a higher granularity.

ACKNOWLEDGEMENT

FUNDING

REFERENCES

1. UITP, *Public transport authorities and COVID-19: impact and response to a pandemic.* https://www.lek.com/sites/default/files/PDFs/COVID19-public-transport-impacts.pdf, 2020, accessed: 2020-05-30.
2. Bucsky, P., Modal share changes due to COVID-19: The case of Budapest. *Transportation Research Interdisciplinary Perspectives*, 2020, p. 100141.
3. Gray, R. S., Agriculture, transportation, and the COVID-19 crisis. *Canadian Journal of Agricultural Economics/Revue canadienne d'agroeconomie*, 2020.
4. Nicola, M., Z. Alsafi, C. Sohrabi, A. Kerwan, A. Al-Jabir, C. Iosifidis, M. Agha, and R. Agha, The socio-economic implications of the coronavirus and COVID-19 pandemic: a review. *International Journal of Surgery*, 2020.
5. Bereitschaft, B. and D. Scheller, How Might the COVID-19 Pandemic Affect 21st Century Urban Design, Planning, and Development? *Urban Science*, Vol. 4, No. 4, 2020, p. 56.
6. Tirachini, A. and O. Cats, COVID-19 and public transportation: Current assessment, prospects, and research needs. *Journal of Public Transportation*, Vol. 22, No. 1, 2020, p. 1.
7. Gkiotsalitis, K. and O. Cats, Public transport planning adaption under the COVID-19 pandemic crisis: literature review of research needs and directions. *Transport Reviews*, Vol. 41, No. 3, 2021, pp. 374–392.
8. Hâncean, M.-G., M. Perc, and J. Lerner, Early spread of COVID-19 in Romania: imported cases from Italy and human-to-human transmission networks. *Royal Society open science*, Vol. 7, No. 7, 2020, p. 200780.
9. Nicotra, I., M. Petri, A. Pratelli, R. R. Souleyrette, and T. A. Wang, Mobility Impacts of the Second Phase of Covid-19: General Considerations and Regulation from Tuscany (Italy) and Kentucky (USA). In *International Conference on Computational Science and Its Applications*, Springer, 2020, pp. 255–268.

10. Gkiotsalitis, K., A model for modifying the public transport service patterns to account for the imposed COVID-19 capacity. *Transportation Research Interdisciplinary Perspectives*, Vol. 9, 2021, p. 100336.

11. Yu, B., Z. Yang, and J. Yao, Genetic algorithm for bus frequency optimization. *Journal of Transportation Engineering*, Vol. 136, No. 6, 2010, pp. 576–583.

12. Szeto, W. Y. and Y. Wu, A simultaneous bus route design and frequency setting problem for Tin Shui Wai, Hong Kong. *European Journal of Operational Research*, Vol. 209, No. 2, 2011, pp. 141–155.

13. Fellesson, M. and M. Friman, Perceived satisfaction with public transport service in nine European cities. In *Journal of the Transportation Research Forum*, 2012, Vol. 47.

14. Gkiotsalitis, K. and F. Alesiani, Robust timetable optimization for bus lines subject to resource and regulatory constraints. *Transportation Research Part E: Logistics and Transportation Review*, Vol. 128, 2019, pp. 30–51.

15. Gkiotsalitis, K., M. Schmidt, and E. van der Hurk, Subline frequency setting for autonomous minibusses under demand uncertainty. *Transportation Research Part C: Emerging Technologies*, Vol. 135, 2022, p. 103492.

16. Ceder, A., Bus frequency determination using passenger count data. *Transportation Research Part A: General*, Vol. 18, No. 5-6, 1984, pp. 439–453.

17. Furth, P. G. and N. H. Wilson, Setting frequencies on bus routes: Theory and practice. *Transportation Research Record*, Vol. 818, No. 1981, 1981, pp. 1–7.

18. Ceder, A., Urban transit scheduling: framework, review and examples. *Journal of urban planning and development*, Vol. 128, No. 4, 2002, pp. 225–244.

19. Sun, S. and W. Szeto, Optimal sectional fare and frequency settings for transit networks with elastic demand. *Transportation Research Part B: Methodological*, Vol. 127, 2019, pp. 147–177.

20. Bertsimas, D., Y. Sian Ng, and J. Yan, Joint Frequency-Setting and Pricing Optimization on Multimodal Transit Networks at Scale. *Transportation Science*, Vol. 54, No. 3, 2020, pp. 839–853.

21. Cipriani, E., S. Gori, and M. Petrelli, Transit network design: A procedure and an application to a large urban area. *Transportation Research Part C: Emerging Technologies*, Vol. 20, No. 1, 2012, pp. 3–14.

22. Ibarra-Rojas, O. J., F. Delgado, R. Giesen, and J. C. Muñoz, Planning, operation, and control of bus transport systems: A literature review. *Transportation Research Part B: Methodological*, Vol. 77, 2015, pp. 38–75.

23. Szeto, W. Y. and Y. Jiang, Transit route and frequency design: Bi-level modeling and hybrid artificial bee colony algorithm approach. *Transportation Research Part B: Methodological*, Vol. 67, 2014, pp. 235–263.

24. Mahdavi Moghaddam, S. H., K. R. Rao, G. Tiwari, and P. Biyani, Simultaneous bus transit route network and frequency setting search algorithm. *Journal of Transportation Engineering, Part A: Systems*, Vol. 145, No. 4, 2019, p. 04019011.

25. Wei, M., T. Liu, B. Sun, and B. Jing, Optimal Integrated Model for Feeder Transit Route Design and Frequency-Setting Problem with Stop Selection. *Journal of Advanced Transportation*, Vol. 2020, 2020.

26.   Verbas, İ. Ö., C. Frei, H. S. Mahmassani, and R. Chan, Stretching resources: sensitivity of optimal bus frequency allocation to stop-level demand elasticities. *Public Transport*, Vol. 7, No. 1, 2015, pp. 1–20.

27.   Verbas, İ. Ö. and H. S. Mahmassani, Exploring trade-offs in frequency allocation in a transit network using bus route patterns: Methodology and application to large-scale urban systems. *Transportation Research Part B: Methodological*, Vol. 81, 2015, pp. 577–595.

28.   Gkiotsalitis, K., Z. Wu, and O. Cats, A cost-minimization model for bus fleet allocation featuring the tactical generation of short-turning and interlining options. *Transportation Research Part C: Emerging Technologies*, Vol. 98, 2019, pp. 14–36.

29.   Liu, T., O. Cats, and K. Gkiotsalitis, A review of public transport transfer coordination at the tactical planning phase. *Transportation Research Part C: Emerging Technologies*, Vol. 133, 2021, p. 103450.

30.   Gkiotsalitis, K. and O. Cats, Reliable frequency determination: Incorporating information on service uncertainty when setting dispatching headways. *Transportation Research Part C: Emerging Technologies*, Vol. 88, 2018, pp. 187–207.

31.   Li, Y., W. Xu, and S. He, Expected value model for optimizing the multiple bus headways. *Applied Mathematics and Computation*, Vol. 219, No. 11, 2013, pp. 5849–5861.

32.   Bellei, G. and K. Gkoumas, Transit vehicles' headway distribution and service irregularity. *Public transport*, Vol. 2, No. 4, 2010, pp. 269–289.

33.   Fu, L. and X. Yang, Design and implementation of bus–holding control strategies with real-time information. *Transportation Research Record*, Vol. 1791, No. 1, 2002, pp. 6–12.

34.   Gkiotsalitis, K. and O. Cats, Optimal frequency setting of metro services in the age of COVID-19 distancing measures. *Transportmetrica A: Transport Science*, 2021, pp. 1–21.

35.   Spiess, H. and M. Florian, Optimal strategies: a new assignment model for transit networks. *Transportation Research Part B: Methodological*, Vol. 23, No. 2, 1989, pp. 83–102.

36.   Nielsen, O. A., A stochastic transit assignment model considering differences in passengers utility functions. *Transportation Research Part B: Methodological*, Vol. 34, No. 5, 2000, pp. 377–402.

37.   Spiess, H., Transit equilibrium assignment based on optimal strategies: an implementation in EMME/2. *EMME/2 Support Center*, 1993.

38.   Spiess, H., Conical volume-delay functions. *Transportation Science*, Vol. 24, No. 2, 1990, pp. 153–158.